

**Advanced Materials
Science and Technology**
ICAMST 2013

Edited by
Kuwat Triyana, Khairurrijal, Risa Suryana,
Heru Susanto and Sutikno



TRANS TECH PUBLICATIONS

Preface

The present volume contains selected papers of the 2013 International Conference on Advanced Materials Science and Technology (ICAMST 2013) held on September 17-18, 2013 in Yogyakarta, Indonesia. The conference, which has been jointly organized by Universitas Gadjah Mada, Institut Teknologi Bandung, Sebelas Maret University, Diponegoro University, and Semarang State University, Indonesia, has accepted more than 330 abstracts. After having reviewed the abstracts, 220 papers were presented in the conference. Finally, under a tight peer-review process by at least two expert referees for each paper, 157 papers were accepted in *Advanced Materials Research*, an international journal indexed by Scopus.

The papers are categorized into several groups that cover new developments and research results related to theoretical and experimental studies of advanced materials as well as their various processing and wide variety of applications. They include nanofibers and membranes, nanoparticles and powders, thick and thin films, biomaterials, electronic materials, magnetic materials, optical materials, composites, ceramics, and alloys as well as measurement and characterization techniques of materials.

Finally, we are grateful to PT. Fajar Mas Murni (Hitachi), PT. Besha Analitika, PT. TEKNOLABindo Penta Perkasa, PT HILAB Sciencetama, PT. Unitama Analitika Perkasa, and PT. Chemoscience Indonesia as sponsors, Indonesian Physical Society (IPS) Yogyakarta & Central Java Chapter, Materials Research Society of Indonesia (MRS-ID), and Physics and Applied Physics Society of Indonesia (PAPSI) for their technical supports, and Trans Tech Publications for producing the volume. Last but not least, we also wish to thank reviewers for invaluable comments and suggestions.

Editors,

Dr. Kuwat Triyana

Department of Physics, Universitas Gadjah Mada (triyana@ugm.ac.id)

Prof. Dr. Khairurrijal

Department of Physics, Institut Teknologi Bandung (krijal@fi.itb.ac.id)

Dr. Risa Suryana

Department of Physics, Sebelas Maret University (rsuryana@uns.ac.id)

Prof. Dr. Heru Susanto

*Department of Chemical Engineering, Diponegoro University
(heru.susanto@undip.ac.id)*

Dr. Sutikno

Department of Physics, Semarang State University (smadnasri@yahoo.com)

Conference Organizers

Universitas Gadjah Mada (UGM), Institut Teknologi Bandung (ITB), Sebelas Maret (UNS), Diponegoro University (UNDIP), and Semarang State University (UNNES)

Table of Contents

Preface and Conference Organizers

Chapter 1: Nanofibers and Membranes

The Role and Prospect of Nanomaterials in Polymeric Membrane for Water and Wastewater Treatment: A State-of-the-Art Overview A.F. Ismail and P.S. Goh	3
Synthesis of Low Fouling Porous Polymeric Membranes H. Susanto, D.P. Julyanti and A. Roihatin	7
Mass Production of Stacked Styrofoam Nanofibers Using a Multinozzle and Drum Collector Electrospinning System M.M. Munir, A.Y. Nuryantini, Iskandar, T. Suciati and K. Khairurrijal	20
Transparent and Conductive Fluorinated-Tin Oxide Prepared by Atmospheric Deposition Technique A. Purwanto	24
Gas Sensing Using Static and Dynamic Modes Piezoresistive Microcantilever R. Nuryadi, L. Aprilia, N. Aisah and D. Hartanto	29
One-Step Fabrication of Short Nanofibers by Electrospinning: Effect of Needle Size on Nanofiber Length I.W. Fathona, K. Khairurrijal and A. Yabuki	33
Carbon Dioxide Permeation Characteristics in Asymmetric Polysulfone Hollow Fiber Membrane: Effect of Constant Heating and Progressive Heating M.A. Bin Azhari, N. Binti Omar, N. Binti Mustaffa and A.F. Ismail	37
Electrospinning of Poly(vinyl alcohol)/Chitosan via Multi-Nozzle Spinneret and Drum Collector A.Y. Nuryantini, M.M. Munir, M.P. Ekaputra, T. Suciati and K. Khairurrijal	41
A Simple Way of Producing Nano Anatase TiO₂ in Polyvinyl Alcohol Fibers Harsojo, K. Triyana and H. Sosiati	45
The Crystal Structure, Conductivity Character and Ionic Migration of Samarium Doped-Ceria (SDC) and its Composite with Sodium Carbonate F. Rahmawati, D.G. Syarif, P.P. Paramita and E. Heraldy	49
Preparation of Sulfonate Grafted Silica/Chitosan-Based Proton Exchange Membrane Z.M. Putrie and H. Setyawan	54
Synthesis and Characterization of Solid Polymer Electrolyte from <i>N</i>-Succinyl Chitosan and Lithium Perchlorate I. Fauzi, I.M. Arcana and D. Wahyuningrum	58
Epoxidised Natural Rubber Based Polymer Electrolyte Systems for Electrochemical Device Applications R. Idris and N.H. Bujang	62
Eggs Shell Membrane as Natural Separator for Supercapacitor Applications E. Taer, Sugianto, M.A. Sumantre, R. Taslim, Iwantono, D. Dahlan and M. Deraman	66
Titania Coated Ceramic Membrane from Clay and Muntilan Sand for Wastewater Filter Application Masturi, E. Sustini, K. Khairurrijal and A. Mikrajuddin	70
Utilization of Fly Ash as Ceramic Support Mixture for the Synthesis of Zeolite Pervaporation Membrane B. Alfyan and H. Susanto	74
Synthesis and Characterization of Nanostructured Tungsten Oxide by Hard Template Method T. Hongo, Y. Usami and A. Yamazaki	78

Chapter 2: Nanoparticles and Powders

Excited-State Proton Transfer in Fluorescent Photoactive Yellow Protein Containing 7-Hydroxycoumarin	
D. Novitasari, H. Kamikubo, Y. Yamazaki, M. Yamaguchi and M. Kataoka	85
Effect of Heating Time on Atrazine-Based MIP Materials Synthesized via the Cooling-Heating Method	
I. Royani, Widayani, A. Mikrajuddin and K. Khairurrijal	89
Preparation of Orange Peel Based Activated Carbons as Cathodes in Lithium Ion Capacitors	
A. Andreas Arie, H. Kristianto, I. Suharto, M. Halim and J.K. Lee	95
Synthesis of Fe₂O₃/C Nanocomposite Using Microwave Assisted Calcination Method	
A.P. Swardhani, F. Iskandar, A. Mikrajuddin and K. Khairurrijal	100
Magnetic CuFe₂O₄ Nanoparticles for Adsorption of Cr(VI) from Aqueous Solution	
P.L. Hariani and F. Riyanti	104
Optical Properties of Zn-Doped CeO₂ Nanoparticles as a Function of Zn Content	
I. Nurhasanah, H. Sutanto and R. Futikhaningtyas	108
Chelating Agent Role in Synthesizing Cerate-Zirconate Powder by a Sol-Gel Method	
N. Osman, N.A. Abdullah and S. Hasan	112
Influence of Ionic Surfactants under Ultrasonic Irradiation to Reduce the Particle Size of Mechanically Alloyed La_{1-x}Sr_xFe_{0.5}Mn_{0.25}Ti_{0.25}O₃ Powders	
M.A.E. Hafizah, A. Manaf and B. Soegijono	116
Covalent Functionalization of Amino Group onto Carbon-Based Magnetic Nanoparticles Using Pulsed-Powder Explosion Technique	
T.E. Saraswati, S. Tsumura and M. Nagatsu	122
Magnetic Properties and Microstructures of Polyethylene Glycol (PEG)-Coated Cobalt Ferrite (CoFe₂O₄) Nanoparticles Synthesized by Coprecipitation Method	
E. Suharyadi, E.A. Setiadi, N. Shabrina, T. Kato and S. Iwata	126
Copper-Zinc-Titania Nanocomposite as Catalyst for CO₂ Photo-Reduction: A Surface Deactivation Study	
O. Zuas, Y.K. Krisnandi, W. Wibowo, J.S. Kim and J. Gunlazuardi	134
The Highly Active Photocatalyst of Silver Orthophosphate under Visible Light Irradiation for Phenol Oxidation	
U. Sulaeman, I.R. Nisa, A. Riapanitra, P. Iswanto, S. Yin and T. Sato	141
Treatment of Coal Stockpile Wastewater by Electrocoagulation using Aluminum Electrodes	
Rusdianasari, Y. Bow and A. Taqwa	145
Preparation of Activated Carbons from Coconuts Shell for Pb (II) Adsorption	
E. Yusmartini, D. Setiabudidaya, Ridwan, Marsi and Faizal	149
Preparation of Sulfated Zirconia Using Modified Sol Gel Method	
A. Kristiani, K.C. Sembiring, F. Aulia, J.A. Laksmono, S. Tursiloadi and H. Abimanyu	153
Enrichment of Indonesian Low Rank Coal's Surface Oxygen Compounds (SOCs) Using Hydrogen Peroxide and its Adsorptive Properties	
G. Yuliani, I. Noviyana and A. Setiabudi	159
Characteristics of Water-ZrO₂ Nanofluids with Different pH Utilizing Local ZrO₂ Nanoparticle Prepared by Precipitation Method	
D.G. Syarif	163
Corrosion of Carbon Steel in Nanofluid Containing ZrO₂ Nanoparticle at Different Temperature	
D.H. Prajitno and D.G. Syarif	168

Chapter 3: Thick and Thin Films

Contact Formation at Interface of LSCO BCZY LSCO Symmetrical Cell: Effect of LSCO to PVP Ratio	
A.A. Samat, S.A. Safri, D. Samsudin, W.S. Jaafar and N. Osman	175
Preparation of Activated Carbon Monolith Electrodes from Sugarcane Bagasse by Physical and Physical-Chemical Activation Process for Supercapacitor Application	
E. Taer, Iwantono, S.T. Manik, R. Taslim, D. Dahlan and M. Deraman	179
The Effect of Paste Preparation and Annealing Temperature of ZnO Photoelectrode to Dye-Sensitized Solar Cells (DSSC) Performance	
A. Syukron, R.A. Wahyuono, D. Sawitri and D.D. Risanti	183

Utilization of Natural Porphyrin Thin Films as a Photosensitizer for Photodetectors Utari, A. Heru Wibowo, B. Purnama and K. Abraha	187
Effect of Growth Temperature on Cobalt-Doped TiO₂ Thin Films Deposited on Si (100) Substrate by MOCVD Technique A. Saripudin, H. Saragih, K. Khairurrijal, Khairurrijal and P. Arifin	192
Fabrication of Aluminum Doped Silica Preform Using MCVD and Solution Doping Technique: Soot Analyses and Solution Concentration Effect S.M. Aljamimi, Z. Yusoff, H.A. Abdul-Rashid, K.M.S. Anuar, S.Z. Muhamad Yassin, M.I. Zulkifli, S. Hanif and N. Tamchek	197
The Influence of Mn/Ga Solution Mole Fraction on the Solid Composition and Microstructure of GaN:Mn Thin Film Deposited on Silicon Substrate by Spin Coating Technique H. Sutanto, I. Nurhasanah, I. Istadi and Priyono	203
Grain Size Analysis on Ba_{0.65}Sr_{0.35}TiO₃ Thin Films Using Design of Experiment V. Retnasamy, Z. Sauli, R. Vairavan, S. Taniselass, M.H. Ab Aziz, P. Ehkan and F.A.A. Fuad	211
Fabrication and Characterization of Stacked Self-Assembled In_{0.5}Ga_{0.5}As/GaAs Quantum Dots Grown by MOCVD D. Aryanto, Z. Othaman and A.K. Ismail	215
Er₂O₃-Al₂O₃ Doped Silica Preform Prepared by MCVD-Chelate Vapor Phase Delivery Technique K.M.S. Anuar, S.Z. Muhd-Yasin, M.I. Zulkifli, S. Hanif, A. Yusoff, S.M. Aljamimi, H.T. Zubair, Z. Yusoff, H.A. Abdul-Rashid and N. Tamchek	219
The Effect of Variation Concentration Nd³⁺ Ions on Physical and Optical Properties of TZBN Glass E. Nurliana, Riyatun and L. Rahmasari	225
Effects of Iron Dopants on Barium Strontium Titanate (Ba_{0.8}Sr_{0.2}TiO₃) Thin Films R.T. Setyadhani, A. Jamaludin and Y. Iriani	229
Wettability Study Using O₂ and Ar RIE Gas Treatment on Aluminium Surface V. Retnasamy, Z. Sauli, M. Palianysamy, S. Taniselass, P. Ehkan and F.A.A. Fuad	233
Room-Temperature Deposition of ZnO Thin Films by Using DC Magnetron Sputtering P. Marwoto, S. Sulhadi, Sugianto, D. Aryanto, E. Wibowo and K. Wahyuningsih	237
Defects Induced by Reactive Ion Etching in Ge Substrate Kusumandari, N. Taoka, W. Takeuchi, M. Sakashita, O. Nakatsuka and S. Zaima	241
Effect of Electrolyte Composition on Corrosion Resistance in Nickel Plating Process for Coating Bonded Magnet PrFeB C. Kurniawan, H.M.A. Sholihat, K.A.Z. Thosin, Muljadi and P. Sardjono	245
Effects of Sputtering Coating Factors on Elastic Modulus of MoN Coatings P. Srisattayakul, C. Saikaew, A. Wisitsoraat and N. Intanon	249
Effect of Anodizing in Surface Finishing on Speed Boat Impeller Made of Aluminum S. Soekrisno and B. Anggoro	253

Chapter 4: Biomaterials

Biomimetic Creation of Surfaces on Porous Titanium for Biomedical Applications K. Mediaswanti, C.E. Wen, E.P. Ivanova, F. Malherbe, C.C. Berndt, V.T.H. Pham and J. Wang	259
Production and Characterization of Biodegradable Plastics Based on Starch of <i>Artocarpus heterophyllus</i> Lam Seeds Sutikno, P. Marwoto and A. Dian Puspita	263
Characteristics of Mg-Ca-Zn Alloy Metallic Foam Based on Mg-Zn-CaH₂ System I. Kartika, Y.N. Thaha, F. Pramuji Lestari and B. Sriyono	267
The Effect of Repeated Impingement on UHMWPE Material in Artificial Hip Joint during Salat Activities J. Jamari, R. Ismail, E. Saputra, S. Sugiyanto and I.B. Anwar	272
Simple and Easy Method to Synthesize Chicken Eggshell Based Hydroxyapatite S. Tri Wahyudi, S. Utami Dewi, A. Anggraeni, K. Dahlan, Akhmaloka, M. Ali Zulfikar and R. Hertadi	276
Synthesis of Chitosan-Gold Nanoparticles for Drug Delivery H. Yazid, A.M. Yassin, A.Z. Ruslan, S.H. Alias, R. Adnan and A.M. Md Jani	280

Synthesis of Hydroxyapatite Nanoparticle from Tutut (<i>Bellamyia javanica</i>) Shells by Using Precipitation Method for Artificial Bone Engineering L. Herawaty, E. Rohaeti, Charlena and S.G. Sukaryo	284
Adsorption of Lead Ions onto Citric Acid Modified Rubber (<i>Hevea brasiliensis</i>) Leaves S. Ibrahim, M.A.K.M. Hanafiah and F. Fadzil	288
Effect of Deacetylation on Characterization of pH Stimulus Responsive Chitosan-Acrylamide Hydrogels Using Radiation K.T. Basuki, D. Swantomo, Sigit and K. Megasari	292
Synthesis of Smart Biodegradable Hydrogels Cellulose-Acrylamide Using Radiation as Controlled Release Fertilizers D. Swantomo, R. Rochmadi, K.T. Basuki and R. Sudiyo	296
Structural Studies of 1,3:2,4-Dibenzylidene Sorbitol Gels H. Takeno and Y. Kuribayashi	300
Effects of Surface Treatments on Nata de Cassava on the Tensile Strength and Morphology of Bacterial Cellulose Sheet D. Cahyandari and H.S. Budi Rohardjo	305
Impact and Thermal Properties of Unsaturated Polyester (UPR) Composites Filled with Empty Fruit Bunch Palm Oil (EFBPO) and Cellulose E. Surya, Michael, Halimatuddahlia and Maulida	310
Biodegradation of Low Density Polyethylene (LDPE) Composite Filled with Cellulose and Cellulose Acetate Halimatuddahlia and A.M. Rambe	314
The Treated Rice Straw as Potentially Feedstock of Wood and Rice Straw Fiber Blend for Pulp and Paper Making Industry A.L. Juwono and S. Handoko	318
Experimental Studies of Thermo-Induced Mechanical Effects in the Main-Chain Liquid Crystal Elastomers Supardi, Harsojo and Y. Yusuf	322
Characterization of Photo Biocomposites for Application in Biomedical Materials j. triyono, A.E. Tontowi, W. Siswomihardjo and R. Rochmadi	327
Study on Ginger Extract Performance as Corrosion Inhibitor in Acid and Neutral Environments B.A. Kurniawan, A. Pradana, Sulistijono and S. Sutarsis	331
Comparison between Slip Casting and Cold Isostatic Pressing for the Fabrication of Nanostructured Zirconia N.F. Amat, A. Muchtar, N. Yahaya, M.J. Ghazali and C.C. Hao	335

Chapter 5: Electronic Materials

Fabrication of Silver Nanoparticles and its Films and their Characterization of Structure and Electrical Conductivity M. Diantoro, A.F. Chasanah, Nasikhudin, N. Mufti and A. Fuad	341
Crystallographic and Electrical Properties of Barium Zirconium Titanate Doped by Indium and Lanthanum S.R. Adnan, M. Hikam and E. Rizky	347
Ohmic Contact in P-HEMT Wafer Using Metallization with Ge/Au/Ni/Au A. Dolah, M.A. Abd Hamid, M. Deraman, A. Yusof, N.A. Ngah and N.F.I. Muhammad	351
Possible Existence of the Stripe Correlations in Electron-Doped Superconducting Cuprates $\text{Eu}_{1.85}\text{Ce}_{0.15}\text{Cu}_{1-y}\text{Ni}_y\text{O}_{4+\alpha-\delta}$ Studied by Muon-Spin-Relaxation R. Risdiana, L. Safriani, W.A. Somantri, T. Saragi, T. Adachi, I. Kawasaki, I. Watanabe and Y. Koike	354
Fabrication and Characterization of Ferroelectric Thin Film $\text{Ba}_x\text{Sr}_{1-x}\text{TiO}_3$ for Application in Light Intensity Detector A. Jamaluddin, E. Susilowati, S. Budiawanti and Y. Iriani	358
A Theoretical Study on Electron Tunneling Current in Isotropic High-κ Dielectric Stack-Based MOS Capacitors with Charge Trapping F.A. Noor, Khairiah, A. Mikrajuddin and K. Khairurrijal	363

Modeling of Drain Current in Armchair Graphene Nanoribbon Field Effect Transistor Using Transfer Matrix Method E. Suhendi, F.A. Noor, N. Kurniasih and K. Khairurrijal	367
A Theoretical Model of Band-to-Band Tunneling Current in an Armchair Graphene Nanoribbon Tunnel Field-Effect Transistor C.S.P. Bimo, F.A. Noor, M. Abdullah and K. Khairurrijal	371
Determination of Thin Film $\text{Ba}_{0.5}\text{Sr}_{0.5}\text{TiO}_3$ Ferroelectric Effective Mass from I-V Characteristics Calculation Using Transfer Matrix Method L. Hasanah, I. Hamidah, A. Hamdani, B. Mulyanti, D. Rusdiana and H. Yuwono	375

Chapter 6: Magnetic Materials

Thermal Analysis and Magnetic Properties of Lanthanum Barium Manganite Perovskite P. Sardjono and A.A. Wisnu	381
Magnetoelectric Coupling Phenomena Based on the Changes of Magnetic Properties in Multiferroic Nanocomposite $\text{BaTiO}_3\text{-BaFe}_{12}\text{O}_{19}$ D. Suastiyanti, B. Soegijono and M. Hikam	385
Microstructural Studies of $(\text{Ba}_{0.7}\text{Sr}_{0.3}\text{Fe}_{12}\text{O}_{19})_{1-x} - (\text{Ba}_{0.7}\text{Sr}_{0.3}\text{TiO}_3)_x$ with $x = 0.2$, $x = 0.5$ and $x = 0.8$ Composite System by Mechanical Alloying Process Novizal, A. Manaf and P. Sardjono	391
Modeling of Magnetorheological Damper Using Back Propagation Neural Network Ubaidillah, G. Priyandoko, M. Nizam and I. Yahya	396
Microstructural and Magnetic Properties of $\text{Ti}^{2+}\text{-Mn}^{4+}$ Substituted Barium Hexaferrite M. Manawan, A. Manaf, B. Soegijono and A. Yudi	401
The Influence of Ni-Doping on Structure and Magnetic Properties of $\text{La}_{0.67}\text{Ba}_{0.33}\text{MnO}_3$ S.S. Ahmiatri, A. Manaf and B. Kurniawan	406
Micromagnetic Study on the Dynamic Susceptibility Spectra of Square-Patterned Ferromagnets D. Djuhana, J.A. Kadir, A.T. Widodo and D.H. Kim	410
Micromagnetic Simulation on Ground State Domain Structures of Barium Hexaferrite ($\text{BaFe}_{12}\text{O}_{19}$) D. Djuhana, D.C.C. Oktri and D.H. Kim	414
Magnetic Properties and Reflection Loss Characteristic of Mn-Ti Substituted Barium-Strontium Hexaferrite V.V.R. Repi, A. Manaf and B. Soegiono	418
Analysis of Structural and Microstructure of Lanthanum Ferrite by Modifying Iron Sand for Microwave Absorber Material Application N. Taufiqu Rochman and A.A. Wisnu	423
Characterization of Single Phase of $\text{La}_{0.8}\text{Ba}_{0.2}\text{Fe}_{0.3}\text{Mn}_{0.35}\text{Ti}_{0.35}\text{O}_3$ Nanoparticles as Microwave Absorbers A. Manaf and A.A. Wisnu	428
Magnetic Properties of Coring Samples from Aceh Basin West Off Sumatera Island E.Z. Gaffar	434
Microwave Properties of Composite $\text{Ba}_{0.5}\text{Sr}_{0.5}\text{Fe}_{11.7}\text{Mn}_{0.15}\text{Ti}_{0.15}\text{O}_{19}/\text{La}_{0.7}\text{Ba}_{0.3}\text{MnO}_3$ Material V.V.R. Repi, A. Manaf and B. Soegiono	440
Experiment Using a Magnetically Controlled Ferrofluid Flow in a Flatplate Laminar Flow System Y.H. Fan, L.Y. Lou and Y.M. Chen	444

Chapter 7: Optical Materials

Anode Buffer for Organic Devices Composed of Gold Nanoparticles Prepared by Ark Plasma Deposition D. Wang, N. Yukitake and K. Fujita	451
A Simple Optimization of Triple-Junction Solar Cell $\text{nc-Si:H/a-Si:H/a-SiGe:H}$ Using Computer Modeling and Robust Design T. Abuzairi and N.R. Poespawati	455

Detailed Analysis of Shallow and Heavily-Doped Emitters for Al-BSF Bifacial Solar Cells S. Sepeai, S.H. Zaidi, M.Y. Sulaiman, K. Sopian, M.A. Ibrahim, M.K.M. Desa and M.D. Norizam	459
Microwave-Assisted Solid State Synthesis of Red-Emitting BCNO Phosphor and its Characteristics B.W. Nuryadin, E.C. Septia, F. Iskandar, T. Ogi, K. Okuyama, A. Mikrajuddin and K. Khairurrijal	464
Synthesized 2,4,5-Triphenylimidazole as Precursor of Organic Light Emitting Diode (OLED) Material I.B. Rachman and D. Wahyuningrum	468
Preliminary Study on the Photovoltaic and Impedance Characteristics of Dye Sensitized Solar Cell (DSSC) using Polymer Gel Electrolyte W.S. Arsyad, H. Pujiarti, P. Wulandari, Herman and R. Hidayat	472
Charge Carrier Dynamics of Active Material Solar Cell P3HT:ZnO Nanoparticles Studied by Muon Spin Relaxation (μSR) L. Safriani, R. Risdiana, A. Bahtiar, A. Aprilia, R.E. Siregar, R. Hidayat, T.P.I. Saragi, I. Kawasaki and I. Watanabe	477
Influence of Mass Ratio of Aquadest and TTIP on the Synthesis of TiO₂ Nanoparticles to Improve the Performance of DSSC with Beta-Carotene as Sensitizer N. Ardhani, A. Supriyanto, A.H. Yuwono and R. Suryana	481
Sol-Gel Derived ZnO Nanorod Templated TiO₂ Nanotube Synthesis for Natural Dye Sensitized Solar Cell I. Kartini, Evana, Sutarno and Chotimah	485
Organic-Inorganic Solar Cell Based on Sprayed MEH-PPV/ZnO Nanorods Layers F.A. Mahmoud, A.B. Shehata, H. Mohamed and W. Magdy	489
Dimensional Analysis of Grid Pattern on a Nematic Liquid Crystal D. Wahyuni, I.R. Kusumawardany, S. Hartini and Y. Yusuf	493
Structural, Chemical Composition and Optical Properties of CdTe Fabricated by Vacuum Evaporation Technique A. Ariswan	497
The Formulation of Phonon as the Result of Second Quantization of Crystalline Lattice Vibration Using Wave Functional Method A. Hermanto	502
Synthesis of Tungsten Oxide (WO₃) Film on Glass Substrate Using Aqueous Based Solution Spray Deposition Method H. Widiyandari, I. Firdaus, A. Purwanto and V.G. Slamet	506
Effect of Oxygen Plasma on the Optical Properties of Monolayer Graphene I. Santoso, R.S. Singh, P.K. Gogoi, T.C. Asmara, D.C. Wei, W. Chen, A.T.S. Wee, V.M. Pereira and A. Rusydi	510

Chapter 8: Composites, Ceramics, and Alloys

The Influence of Sandblasting and Electropolishing on the Surface Hardness of AISI 316L Stainless Steel Suyitno and Ishak	517
Ground Shear Strain and Rate of Erosion in the Coastal Area of North Bengkulu, Indonesia M. Farid, K. Sri Brotopuspito, Wahyudi, Sunarto and W. Suryanto	521
Preparation and Characterization of Magnetite-Silica Nano-Composite as Adsorbents for Removal of Methylene Blue Dyes from Environmental Water Samples A. Fisli, S. Yusuf, Ridwan, Y.K. Krisnandi and J. Gunlazuardi	525
Development of Hydrocracking Catalyst Support from Kaolin of Indonesian Origin E.S. Rahayu, T.W. Samadhi, S. Subagjo and M.L. Gunawan	532
Adsorption Mechanism of Carbon Monoxide on PtRu and PtRuMo Surfaces in the Density Functional Theory Perspective W.T. Cahyanto	537
ZnO-SiO₂/Laponite Photocatalyst: Kinetic Study on Photocatalytic Decolorization of Methylene Blue I. Fatimah and N.N. Yuyun	541

Hydrothermal Synthesis and Visible-Light-Driven Photocatalytic Activity of Allophane – Wakefieldite-(Ce) Composite	
M. Hojamberdiev, Y. Makinose, K. Katsumata, T. Isobe, N. Matsushita and K. Okada	545
Study of Internal Response of Epoxy due to Compressive Load via Experiment and Simulation Using Abaqus FEA Software	
I.D. Aditya, Widayani, S. Viridi and S.N. Khotimah	549
Development of Geopolymer Utilizing Inorganic Waste Materials	
T.W. Samadhi, P.P. Pratama and N. Muan	553
High Compressive Strength of Palm Oil Empty Fruit Bunches (<i>Elaeis guineensis</i>) Composites	
I. Sriyanti, L. Agustina, I. Selviana and L. Marlina	557
Improving the Physico-Mechanical Properties of Eco-Friendly Composite Made from Bamboo	
R. Widyorini, A. Puspa Yudha, R. Isnain, A. Awaluddin, T. Agus Prayitno, A. Ngadianto and K. Umemura	562
Properties of the Treated Kenaf/Polypropylene (PP) Composites	
H. Sosiati, Supatmi, D.A. Wijayanti, R. Widyorini and Soekrisno	566
Improving Mechanical Properties of Ceramic Composites by Harmonic Microstructure Control	
L. Anggraini, R. Yamamoto, K. Hagi, H. Fujiwara and K. Ameyama	570
Application of Carbon Fiber-Based Composite for Electric Vehicle	
M. Anwar, I.C. Sukmaji, W.R. Wijang and K. Diharjo	574
Coating Steel with Nanosilica by Pulsed Direct Current Electrophoresis for Corrosion Protection	
S.N.M.I. Putri and H. Setyawan	578
<i>In Situ</i> Al/Al₂O₃ Composite Coating on Steel Substrate Prepared by Mechanical Alloying at High Temperature	
A.S. Wismogroho and W.B. Widayatno	582
Nano-Micro Characterization of NiCoCrAl Coating on Carbon Steel Substrate	
S. Eni, K. Zaini, Y.M. Wang, N. Hashimoto, S. Hayashi and S. Ohnuki	586
Influence of Sintering Temperature on the Translucency of Sintered Zirconia by Cold Isostatic Pressing	
C.H. Chin, A. Muchtar, N.F. Amat, M.J. Ghazali and N. Yahaya	591
The Phenomenon of Pitting Corrosion Attack on the Milled Aluminium Alloy Al 2618 Plate during Surface Preparation through Sulphuric Acid Anodising	
H. Subawi and Sutarno	596
Study of Laser Cladding of Stellite 6 on Nickel Superalloy Substrate with Two Different Energy Inputs	
A. Kusmoko, D. Dunne, H.J. Li and D. Nolan	600
Interdiffusion of Elements in Aluminum 2024 Clad during Reheat Treatment Process at 495°C	
E. Basuki, Sutarno and Samuel	605
Boron Carbide B₂₅C and B₈C₁₈ Synthesized Using Boric Acid-Glucose and Boric Acid-Active Carbon at Low Temperature without Coreductor Materials	
M.C.F. Toana and B. Soegijono	609
Influence of Oxygen on Microstructures of Ti-Mo-Cr Alloy	
J. Syarif, E. Kurniawan, M.R. Rasani, Z. Sajuri, M.Z. Omar and S. Harjanto	613
Effect of Copper Addition on the High Temperature Oxidation of Zirconium Alloy ZrNbMoGe for Advanced Reactor Fuel Cladding Material	
B. Bandriyana, D.H. Prajitno and A. Dimiyati	617
Fractographic Analysis of 5052 Al-Mg Alloys Processed by Equal Channel Angular Pressing	
E. Mabururi and I.N.P.A. Gede	621
Fatigue and Mechanical Properties of Aluminium-Copper Bi-Metal Tubes	
Z. Sajuri, A. Baghdadi, M.F. Mahmud and J. Syarif	626

Chapter 9: Measurement and Characterization Techniques

Determination of Band Gap Energy of Semiconductor in Homojunction Structure Devices by Using Customized Microcontroller Based Apparatus K. Triyana, S. Ramadhan, A.M.I. Barata, Chotimah and Harsojo	633
Macrotexture Study of Non- and Sintered Pure Nb and Nb₃Sn Using Orientation Distribution Function K. Aniswatin, D.D. Risanti and A.W. Pramono	638
Modeling of Repeated Rolling Contact on Rough Surface: Surface Topographical Change R. Ismail, E. Saputra, M. Tauviqirrahman, J. Jamari and D.J. Schipper	642
Neutron Diffraction Measurements on Dissimilar Metal Weld of Cu-Al Obtained by Friction Stir Welding Method T.H. Priyanto, Bharoto, R. Muslih and H. Mugirahardjo	646
Testing of Materials for Heat and Moisture Transport V. Dvořák, P. Novotny and T. Vít	650
Simultaneous Calibration for MEMS Gyroscopes of the Rocket IMU Wahyudi, A. Susanto, W. Widada and S.P. Hadi	656
Quantitative Bump Height Analysis in ENIG Using Design of Experiment Z. Sauli, V. Retnasamy, P. Ehkan, F.A.A. Fuad and A.K.T. Yeow	660
Automation of Four Circle Diffractomete /Texture Diffractometer for Studies of Crystal Structure and Texture Measurements Bharoto, A. Ramadhani, N. Suparno and T.H. Priyanto	664
Celluloide Film Based Infrared Bandpass Filter for Thermography Kusminarto and U. Pratiwi	668
Comparison between Automatic and Semiautomatic Thresholding Method for Mammographic Density Classification S. Uyun, S. Hartati, A. Harjoko, Subanar and L. Choridah	672
Image Processing for Multiple Micro-Radiography Images A.C. Louk, G.B. Suparta and N. Hidayah	676
3D Micro-Radiography Imaging for Quick Assessment on Small Specimen G.A. Wiguna, G.B. Suparta and A.C. Louk	681
Effect of EDTA and PYP as Co-Ligand of Radiolabeled Nanomaterial M41S-NH₂ for Radiosynovectomy I. Daruwati, M.P. Christina, W.W. Perdana, N.W. Hakiki and N.K. Oekar	687
Weld Defect Classification in Radiographic Film Using Statistical Texture and Support Vector Machine Muhtadan, R. Hidayat, Widyawan and F. Amhar	695
Investigation of Moisture in Coal Using Electrical Capacitance Volume Tomography I. Maulana, D. Haryono, W.P. Taruno, M. Al Huda, M. Baidillah and R.I. Sulaiman	701
Design and Fabrication of Wear Testing Machine for a Fishing Net-Weaving Machine Component N. Intanon, C. Saikaew and P. Srisattayakul	706
High Performance Current-Voltage Characterization System for High Resistance Materials M.M. Munir, Y. Supriadani, M. Budiman and K. Khairurrijal	710
Online Monitoring of Copper Leaching Process Heterogeneity Using Electrical Capacitance Volume Tomography D. Haryono, H. Nugraha, W.P. Taruno, M.R. Baidillah, R.I. Sulaiman and M. Al Huda	714
High Sensitivity Fluxgate Sensor for Detection of AC Magnetic Field: Equipment for Characterization of Magnetic Material in Subsurface W. Indrasari, M. Djamal, W. Srigutomo and N. Hadziqoh	718
Flaw Detection in Welded Metal Using Magnetic Induction Tomography D. Sutisna, S. Ullum, W.P. Taruno, A.A.S. Iman, M.R. Baidillah, M. Al Huda, R.I. Sulaiman and D. Haryono	722
A New Type of Planar Chamber for High Frequency Ozone Generator System M. Facta, Z. Salam and Z. Buntat	726

Magnetic CuFe_2O_4 Nanoparticles for Adsorption of Cr(VI) from Aqueous Solution

Poedji Loekitowati Hariani^{1,a}, Fahma Riyanti^{2,b}

^{1,2}Department of Chemistry, Faculty Mathematics and Science

Sriwijaya University, Palembang, Indonesia

^apujilukitowati@yahoo.com, ^bfatechafj@yahoo.com

Keywords: magnetic CuFe_2O_4 , co-precipitation, adsorption, Cr(VI).

Abstract. CuFe_2O_4 nanoparticles were synthesized by co-precipitation method from the solution of CuCl_2 and FeCl_3 in alkaline condition. The prepared magnetic CuFe_2O_4 can be used to adsorb Cr(VI) ions from aqueous solution and separated from medium by magnetic technique. The characterization of CuFe_2O_4 with X-Ray diffraction (XRD) showed cubic units shells with diameter in the range 15-20 nm which obtained by Transmission Electron Microscope (TEM). The saturation of magnetization was around 13 emu g^{-1} measured with Vibrating Sample Magnetometer (VSM). Batch adsorption studies were carried out to optimize adsorption condition. Effective conditions for adsorption of Cr(VI) were found at the weight of CuFe_2O_4 was 1.0 g with contact time of 60 minutes and pH 3 with adsorption capacity 9.20 mg g^{-1} .

Introduction

Heavy metals in the environment are problem that cannot be resolved until now. Various treatments such as coagulation, precipitation, sedimentation, ultrafiltration, ozonation, electrochemical, and reverse osmosis had been applied to remove heavy metal in solution. One of heavy metal pollutants in the environment is chromium. Chromium has wide applicability in the steel and alloy industries. Chromium species exist mainly in two different oxidation states in water environment, Cr(VI) and Cr(III) ions [1]. Cr(VI) and Cr(III) have contrast different in physiological effects. Cr(III) is essential for human beings [2], and necessary for maintenance of glucose, lipid and protein metabolism in mammals [1], but Cr(VI) can be toxic for biological system, carcinogenic in humans and mutagens and teratogens in biological system [3,4]. Exposure to Cr(VI) and its compounds cause irritation to skin, resulting dermatitis and ulcer formation [2,5]. It has been reported that Cr(VI) is about 500 times more toxic than Cr(III) and the common concentration of Cr(VI) found in wastewater are around 50-100 mg/L [6]. According to EU and WHO standards the maximum total chromium content in drinking water is 0.05 mg L^{-1} [5]. Therefore, developing techniques to removal Cr(VI) from wastewater is an important.

There are several methods used to treat wastewater which contain Cr(VI), such as reduction [7], adsorption [6, 8, 9], and extraction [10]. Adsorption has obtained favor in recent years due to proven efficiency in the removal pollutants from wastewater because availability, profitability, ease of operation and economic. Ferrites of type MFe_2O_4 (M is a different metal cation) have been exploited for wastewater treatment and resulting excellent adsorptive properties with capability of effective recovery by a magnetic separation technique [11]. Ferrites is also known to its excellent chemical stability [12]. Magnetic nanoparticles have large surface area also easy and inexpensive to synthesize [13]. In this study, copper ferrite (CuFe_2O_4) was prepared and the adsorption of Cr(VI) ions were demonstrated. Interaction of magnetic nanoparticles with Cr(VI) caused by attractive electrostatic is influenced by pH solution [8].

Experimental Procedures

Analytical grade CuCl_2 , FeCl_3 and $\text{K}_2\text{Cr}_2\text{O}_7$ were obtained from Merck. CuFe_2O_4 was prepared by co-precipitation method. Prepare 400 mL solution consisting of 0.02 mole of $\text{CuCl}_2 \cdot 2\text{H}_2\text{O}$ and

0.04 mole FeCl_3 at room temperature under vigorous magnetic stirring, slowly raised the pH by adding NaOH (5 mole L^{-1}) up to about 10. Stirring was continued for 30 minutes and the suspension was heated to $95\text{--}100^\circ\text{C}$ for 2 h [6,14]. Synthesis of CuFe_2O_4 reaction[14]:



After cooling, the prepared CuFe_2O_4 was repeatedly washed with distilled water until the pH is neutral. By simple magnetic procedure, the obtained materials were separated from water and dried in oven at 105°C . The crystalline structure of CuFe_2O_4 was determined using X-Ray diffraction Shimadzu XD-610 with $\text{Cu K}\alpha$ radiation in the 2θ range $10\text{--}80^\circ$, Transmission Electron Microscope JEOL JEM 1400 and Vibrating Sample Magnetometer Lakeshore 74004.

Batch adsorption studies were performed by mixing CuFe_2O_4 particles with 100 mL of the 100 mg L^{-1} Cr(VI) ions solution in a flask. This process was carried out using shaker at a constant speed of 120 rpm. All adsorption experiment was carried out at a fixed temperature of $25^\circ\text{C} \pm 1$. The effect of weight of CuFe_2O_4 on the adsorption capacity was studied using weight variation from 0.8 to 1.2 g at pH 5 and contact time of 75 minutes. The effect of pH on the adsorption capacity was studied with pH adjustment from 3 to 8 using 0.1 M HCl and 0.1 M NaOH solutions. The contact time for adsorption process varied at 15, 30, 45, 60 and 75 minutes. Determination of Cr(VI) ions in solution used Atomic Absorption Spectroscopy (AAS) Shimadzu AA-6300 at 540 nm.

Result and Discussion

Characterization of CuFe_2O_4 .

Fig.1 show XRD patterns of CuFe_2O_4 , indicated that the metal oxides can be indexed on a cubic structure. Nine characteristic peaks at 18.7° , 30.2° , 35.6° , 37.2° , 43.6° , 57.1° , 62.8° , 74.5° , and 79.5° were corresponding to the (111), (220), (311), (222), (400), 511), (440), (533) and (440) crystal planes of CuFe_2O_4 [15].

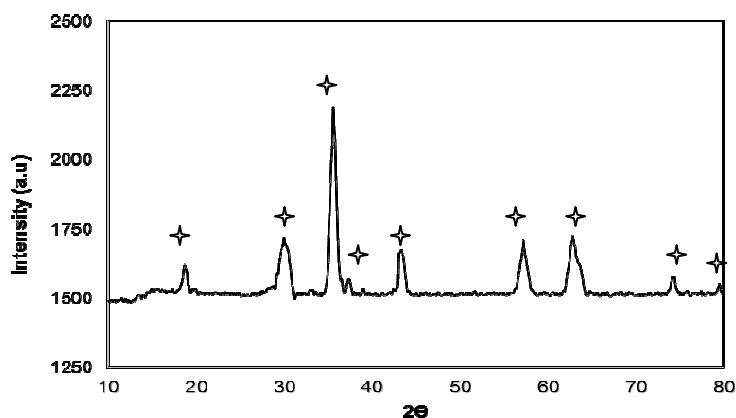


Figure 1. XRD pattern of CuFe_2O_4

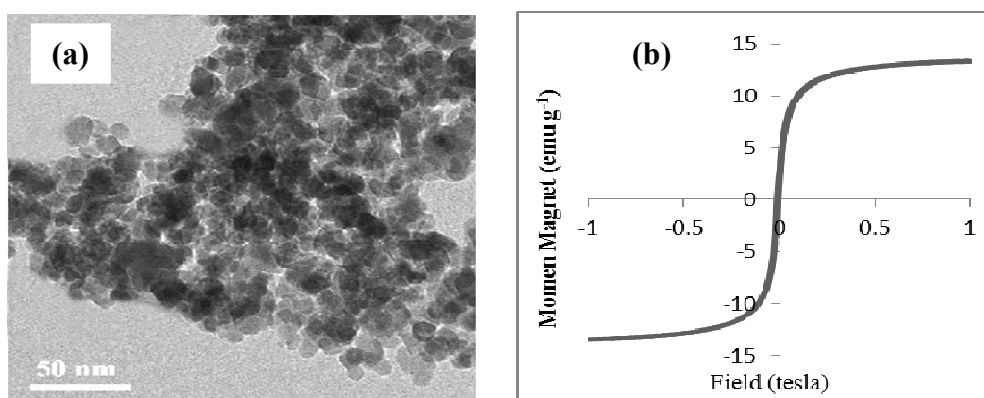


Figure 2. Characteristics of the CuFe_2O_4 by (a) TEM and (b) VSM

Fig. 2 (a) shows TEM image of CuFe_2O_4 , the particle size of the CuFe_2O_4 was found about 15 to 20 nm. Hence, the prepared CuFe_2O_4 by co-precipitation method is found to be nanophase. Fig. 2 (b) show the saturation of magnetization of CuFe_2O_4 was 13 emu g^{-1} . Saturation of magnetization obtained is smaller than the standard saturation magnetization of CuFe_2O_4 as 22.5 emu g^{-1} at room temperature [16].

Optimum adsorption condition. Fig. 3 (a) shows the weight adsorbed of Cr(VI) (mg g^{-1}) with change in the weight of CuFe_2O_4 . It can be observed that the adsorption capacity of Cr(VI) increased with an increased in the weight of CuFe_2O_4 nanoparticles. After equilibrium, the adsorption capacity of Cr(VI) decreased because the weight of CuFe_2O_4 increased but amount of Cr(VI) is limited. Effective weight was found at 1 g CuFe_2O_4 with the adsorption capacity 8.20 mg g^{-1} .

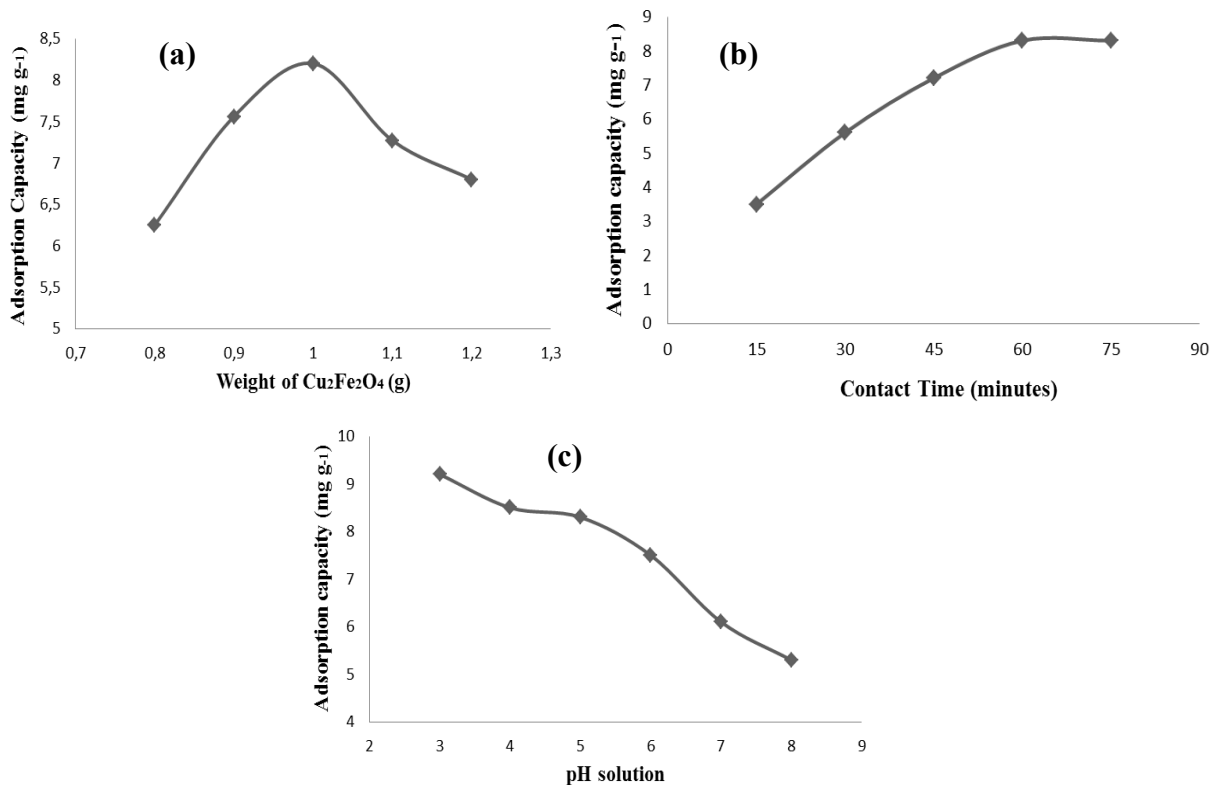


Figure 3. Adsorption capacity by varying of (a) weight CuFe_2O_4 (b) contact time and (c) pH solution

Fig. 3 (b) shows the effect of contact time on the adsorption capacity of Cr(VI). It can be seen that the adsorption process consist of two steps. In the first step, the adsorption capacity rate was at 0 to 60 minutes. The second step, the adsorption capacity was constant at 60 to 75 minutes. The effective contact time was found at 60 minutes with adsorption capacity 8.3 mg g^{-1} . The pH of solution plays an important role in the whole adsorption process and particularly on the adsorption capacity. The effect of pH on adsorption capacity of Cr(VI) arose apparently from the charge properties of both Cr(VI) ions and CuFe_2O_4 . Fig. 3 (c) shows the effect of pH solution on the adsorption capacity of Cr(VI). The maximum of adsorption capacity was observed at pH 3 with adsorption capacity as 9.20 mg g^{-1} . At pH solution $< \text{pH}_{\text{pzc}}$ CuFe_2O_4 (6.3-6.8) adsorbent surface could be positively charged due to the adsorption of H^+ . Therefore, Cr(VI) at the pH from 2 to 6.5 exists mainly in the soluble forms of HCrO_4^- and $\text{Cr}_2\text{O}_7^{2-}$ [6] so the anions are adsorbed by electrostatic attraction.

The adsorption capacity of CuFe_2O_4 to Cr(VI) was smaller when compared to the reduction method using H_2SO_4 and modified chitosan [7,9] but CuFe_2O_4 has the advantage such as it does not

require filtration and adsorption time was faster. The adsorption capacity of CuFe_2O_4 was calculated 9.20 mg g^{-1} . This value is not different with using Fe_3O_4 nanoparticles as 9.7087 mg g^{-1} [8].

Conclusions

Magnetic CuFe_2O_4 nanoparticles were successfully prepared by a chemical co-precipitation method, have cubic phase formed with 15-20 nm diameters size and magnetic saturation as 13 emu g^{-1} . The result of batch experiment for adsorption 100 mL of Cr(VI) with a initial concentration 100 mg g^{-1} showed that the optimum adsorption condition at weight of CuFe_2O_4 1 g, solution pH 3 and contact time of 60 minutes with adsorption capacity as 9.20 mg g^{-1} .

References

- [1] J. Kotas, and Z. Stasicka, Chromium occurrence in the environment and methods of its speciation, *Environ. Pollut.* 107 (2000) 263-268
- [2] F.W. Oehme, In toxicity of heavy metals in the environment, Marcel Dekker Inc., New York, 1979
- [3] A.K. Shanker, C. Cervantes, L. Tavira, S. Avudainayagam, Chromium toxicity in plant, *Environ. Int.* 31 (2005) 739-753
- [4] A. Zhitkovich, Important of chromium DNA adducts in mutagenicity and toxicity in chromium(VI), *Chem. Res. Toxicol.* 18 (2005) 3-11
- [5] N.I. Sax, In Dangerous Properties Of Industrial material, 6th ed., Van Nostrand Reinhold Co, New York, 1984
- [6] Yong, G.Z., H.Y. Shen, S.D. Pan, M.Q. Du and Q.H. Xia, Preparation and characterization of amino functionalized nano- Fe_3O_4 magnetic polymer adsorbents for removal of chromium (VI) ions, *J. Metr. Sci.* 45 (2010) 5291-5301
- [7] P.L. Hariani, H. Nurlisa, Reduction of Cr(VI) ions in aqueous used FeSO_4 , *J. Science Research* 12 (2009) 17-22
- [8] S.H. Dewi, and Ridwan, Synthesis and characterization magnetic nanoparticles Fe_3O_4 for adsorption chromium hexavalen, *Indonesian Journal of Material Science*, 13 (2012) 136-140
- [9] J. Dai, F.L. Ren and C.Y. Tao, Adsorption of Cr(VI) and speciation of Cr(VI) and Cr(III) in aqueous solution using chemically modified chitosan, *Int. J. Environ. Res. Public Health*, 9 (2012) 1757-1770
- [10] Y. Okamoto, Y. Nomura, K. Iwamaru, High preconcentration of ultra trace metal ions by liquid-liquid extraction using water/oil/water emulsion of liquid surfactans membranes, *Microchem. Jour.*, 65 (2000) 341-346
- [11] G. Zhang, J. Qu, H. Liu, R. Liu, R. Wu, Preparation and evaluation of a novel Fe-Mn binary oxide adsorbent for effective arsenite removal, *Water Res.* 41 (2007) 1921-1928
- [12] X. Liu, M., Fu, S. Y., Zhu, L. P., High-yield synthesis and characterization of monodisperse sub-microsized CoFe_2O_4 octahedra. *J. Solid State Chem.* 180 (2007) 461-466
- [13] M. Namdeo and Bajpai, S.K., Chitosan coated nanocomposite (CMNs) as magnetic carrier particles for removal Fe(III) from aqueous solutions, *Colloid Surface* 320 (2008) : 161-168
- [14] S. Hashemian, Kinetic and thermodynamic of adsorption of methylene blue by CuFe_2O_4 /rice bran composite, *Int. J. Physic.Sci.* 6 (2011) 6257-6267
- [15] JCPDS card 25-283, International center for diffraction data, Swathmore, PA, 1986
- [16] H.M. Lu, W.T. Zheng, and Q. Jiang, Saturation magnetization of ferromagnetic and ferrymagnetic nanocrystal at room temperature, *J. Phys. D. Appl.* 40 (2007) 320-325

Magnetic CuFe₂O₄ Nanoparticles for Adsorption of Cr(VI) from Aqueous Solution

10.4028/www.scientific.net/AMR.896.104

DOI References

[1] J. Kotas, and Z. Stasicka, Chromium occurrence in the environment and methods of its speciation, *Environ. Pollut.* 107 (2000) 263-268.

[http://dx.doi.org/10.1016/S0269-7491\(99\)00168-2](http://dx.doi.org/10.1016/S0269-7491(99)00168-2)

[3] A.K. Shanker, C. Cervantes, L. Tavira, S. Avudainayagam, Chromium toxicity in plant, *Environ. Int.* 31 (2005) 739-753.

<http://dx.doi.org/10.1016/j.envint.2005.02.003>

[4] A. Zhitkovich, Important of chromium DNA adducts in mutagenicity and toxicity in chromium(VI), *Chem. Res. Toxicol.* 18 (2005) 3-11.

<http://dx.doi.org/10.1021/tx049774+>

[11] G. Zhang, J. Qu, H. Liu, R. Liu, R. Wu, Preparation and evaluation of a novel Fe-Mn binary oxide adsorbent for effective arsenite removal, *Water Res.* 41 (2007) 1921-(1928).

<http://dx.doi.org/10.1016/j.watres.2007.02.009>

[16] H.M. Lu, W.T. Zheng, and Q. Jiang, Saturation magnetization of ferromagnetic and ferrymagnetic nanocrystal at room temperature, *J. Phys. D. Appl.* 40 (2007) 320-325.

<http://dx.doi.org/10.1088/0022-3727/40/2/006>